Molecular model of hydrophobic solvation

ARTICLE *in* THE JOURNAL OF CHEMICAL PHYSICS · OCTOBER 1999

Impact Factor: 2.95 · DOI: 10.1063/1.480133

3 AUTHORS, INCLUDING:

A. D. J. Haymet
University of California, San Diego
201 PUBLICATIONS **6,440** CITATIONS
SEE PROFILE

Ken A Dill
Stony Brook University
390 PUBLICATIONS **27,536** CITATIONS
SEE PROFILE

Molecular model of hydrophobic solvation

Kevin A. T. Silverstein, A. D. J. Haymet, and Ken A. Dill

Citation: The Journal of Chemical Physics **111**, 8000 (1999); doi: 10.1063/1.480133
View online: http://dx.doi.org/10.1063/1.480133
View Table of Contents: http://scitation.aip.org/content/aip/journal/jcp/111/17?ver=pdfcov
Published by the AIP Publishing

Molecular model of hydrophobic solvation

Kevin A. T. Silverstein[a)]
Graduate Group in Biophysics, University of California, San Francisco, California 94143-0448

A. D. J. Haymet[b)]
Department of Chemistry, University of Houston, Houston, Texas 77204-5641

Ken A. Dill[b),c)]
Department of Pharmaceutical Chemistry, University of California, San Francisco, California 94143-1204

(Received 4 May 1999; accepted 5 August 1999)

The physical basis for the ''hydrophobic effect'' is studied using a simple statistical mechanical model of water, the ''MB'' model, in which water molecules are represented as Lennard-Jones disks with hydrogen bonding arms. Using a four-state framework developed by Muller [Acc. Chem. Res. **23**, 23 (1990)], and extended by Lee and Graziano [J. Am. Chem. Soc. **118**, 5163 (1996)], we find the model reproduces the fingerprints of hydrophobicity, namely, the large positive heat capacity, and temperatures T_H and T_S at which the enthalpy and entropy of transfer, respectively, are zero. Further, the behavior can be interpreted readily in terms of hydrogen bonds that are either made or broken in the bulk or in the first solvation shell around a nonpolar solute. We find that inserting a nonpolar solute into cold water causes ordering and strengthening of the H bonds in the first shell, but that the reverse applies in hot water. This provides a physical interpretation for the crossover temperatures T_H and T_S. © *1999 American Institute of Physics.* [S0021-9606(99)51141-0]

I. KEY TO HYDROPHOBIC THERMODYNAMICS: ΔC_p, T_H, AND T_S

The hydrophobic effect is poorly understood. Hydrophobic solvation refers to the anomalous thermodynamics of transferring a nonpolar solute into water: a large positive free energy, dominated by a large negative entropy around room temperature, and a large positive heat capacity. The heat capacity is the most fundamental of these properties, because it applies over a broad temperature range, and the others can be derived from it. Considerable insight into the nature of hydrophobicity arises from computer simulations,[1–10] integral equation theory,[11–14] scaled-particle theory,[15–18] information theory,[8,19] nuclear magnetic resonance (NMR) experiments,[20–23] and neutron diffraction.[24] However such studies have not yet shed sufficient light on the key quantity, the heat capacity. Some progress toward achieving this goal was made in the recent work by Madan and Sharp,[25,26] who used the random network model[27–30] to calculate transfer heat capacities. These authors performed separate simulations using all-atom Monte Carlo to obtain distributions of water–water bond angles and lengths. Our aim here is to develop an approach which is simpler and yields both the microscopic structure and the macroscopic heat capacity from the same model.

If, in addition to the heat capacity, one also knew the physical basis for the temperatures, T_H and T_S, where the enthalpy and entropy of transfer equal zero,[31–33] then the temperature dependence of hydrophobic solvation would be described, since the free energy may be expressed as

$$\begin{aligned}\Delta G(T) &= \Delta H - T\Delta S \\ &= \Delta H(T_H) - T\Delta S(T_S) + \int_{T_H}^{T} \Delta C_p dT \\ &\quad - T\int_{T_S}^{T} (\Delta C_p/T) dT, \end{aligned} \tag{1}$$

where T is the absolute temperature, and ΔH, ΔS, and ΔC_p are the enthalpy, entropy, and constant-pressure heat capacity of transfer, respectively.

Among several others in the vast literature on the topic are two classes of models that have been widely used to describe the hydrophobic effect. First, all-atom simulations have been an important source of insight into water properties. But due to limitations of current computational power, it has been difficult to achieve numerical convergence for properties as subtle as the heat capacity. Second, there have been thermodynamic models, such as ''mixture models,'' which assume that water has a number of discrete states, with hydrogen bonds that are either made or broken (some of these models are listed in Ref. 34). These too have provided very useful insights, but such models[33,34] have many adjustable parameters, so their physical bases are not always clear.

Here we take an alternative approach. We use a model of water, the MB model,[35,36] for which the statistical mechanics can be explored completely, and which has been shown to have the interesting and anomalous properties of water.[36] This model is simple enough that we can obtain complete convergence of subtle properties, including the heat capacity.

From our MB model simulations, we collect statistics on water distributions, positions, and orientations, which we can

[a)]Present address: Computational Biology Centers, Academic Health Center, University of Minnesota, Box 43 Mayo Bldg., 420 Delaware St. SE, Minneapolis, MN 55455-0312.
[b)]Author to whom correspondence should be addressed.
[c)]Electronic mail: dill@zimm.ucsf.edu

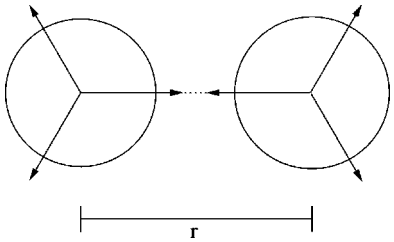

FIG. 1. Two H-bonded MB water molecules, separated by a distance $r = r_{\mathrm{HB}}$, where r_{HB} is the optimal hydrogen-bond distance.

then relate to the thermodynamic properties of the model. However, at the same time, we also find that a very simple two-state model, originated by Muller[33] and modified by Lee and Graziano,[38] provides very illuminating structural insights into ''made'' and ''broken'' bulk and shell hydrogen bonds. Even though the MB model involves continuous distributions, water hydrogen bonding can nevertheless be meaningfully classified into these four types of states. Doing so provides useful insights into hydrophobic thermodynamics of the MB model. The H-bond fractions from our Monte Carlo simulations of the MB model are used directly to obtain parameters for the Muller model, which then are used to compute heat capacities within the Muller framework. The heat capacities computed from the Muller model can be compared directly to the Monte Carlo heat capacities. This leads to a self-consistent verification scheme for the Muller model prediction. Results of the MB-derived parameters are discussed in Secs. III and IV. Finally, in the Appendix we perform exhaustive grid enumerations to study many-body aspects of hydrophobicity.

II. INTERPRETING MB MODEL SIMULATIONS USING THE MULLER FRAMEWORK

A. Review of the MB model

We use the MB model[36] of water, called this because of the resemblance of each model water molecule to the Mercedes–Benz logo. Water molecules are modeled by two-dimensional Lennard-Jones (LJ) disks in a donor and acceptor approximation, with three hydrogen bonding arms that can align with arms of neighboring water molecules (see Fig. 1).

The potential of interaction between two water molecules is given by the sum of two terms:

$$U(\mathbf{X_i},\mathbf{X_j}) = U_{\mathrm{LJ}}(r_{ij}) + U_{\mathrm{HB}}(\mathbf{X_i},\mathbf{X_j}), \tag{2}$$

where, using Ben-Naim's original notation,[35] $\mathbf{X_i}$ denotes the vector representing both the coordinates and the orientation of the ith particle, and r_{ij} is the distance between the molecular centers of particles i and j. The LJ term is customarily written as

$$U_{\mathrm{LJ}}(r_{ij}) = 4\epsilon_{\mathrm{LJ}}\left[\left(\frac{\sigma_{\mathrm{LJ}}}{r_{ij}}\right)^{12} - \left(\frac{\sigma_{\mathrm{LJ}}}{r_{ij}}\right)^{6}\right], \tag{3}$$

where ϵ_{LJ} and σ_{LJ} are the well depth and contact parameters, respectively.

The hydrogen bond is defined to be optimal at a specified distance and relative orientation of the two participating molecules:

$$U_{\mathrm{HB}}(\mathbf{X_i},\mathbf{X_j}) = \epsilon_{\mathrm{HB}} G(r_{ij} - r_{\mathrm{HB}}) \times \sum_{k,l=1}^{3} G(\hat{\mathbf{i}}_k \cdot \hat{\mathbf{u}}_{ij} - 1) G(\hat{\mathbf{j}}_l \cdot \hat{\mathbf{u}}_{ij} + 1). \tag{4}$$

In this expression, the minimum energy ϵ_{HB} corresponds to an idealized hydrogen bond configuration in which one arm of molecule i aligns with an arm of molecule j, and the two molecules' centers are separated by a distance r_{HB}. The unit vector $\hat{\mathbf{i}}_k$ represents the kth arm of the ith particle ($k = 1,2,3$) and $\hat{\mathbf{u}}_{ij}$ is the unit vector joining the center of molecule i to the center of molecule j. The parameters $\epsilon_{\mathrm{HB}} = -1$ and $r_{\mathrm{HB}} = 1$ define the optimal hydrogen bond energy and bond length, respectively. Deviations from this lowest-energy hydrogen-bond configuration (in relative interparticle separation or angle) are described by the unnormalized Gaussian function, $G(x)$, with a single width parameter, σ, for all degrees of freedom:

$$G(x) = \exp(-x^2/2\sigma^2). \tag{5}$$

All energies and temperatures are reported in reduced units, normalized to the strength of the optimal hydrogen bond, ϵ_{HB} (e.g., $T^* = k_B T/\epsilon_{\mathrm{HB}}$, $H^* = H/\epsilon_{\mathrm{HB}}$). Likewise, all distances are scaled by the length of an idealized-hydrogen bond separation, r_{HB} (e.g., $V^* = V/r_{\mathrm{HB}}^2$). The interaction energy, ϵ_{LJ} is one tenth of ϵ_{HB}, and the LJ contact distance is 0.7 that of r_{HB}. The width of the Gaussian is $\sigma = 0.085$. These are the same parameters reported elsewhere.[36]

Constant-pressure Monte Carlo sampling has shown that this model qualitatively predicts the volumetric anomalies of pure water. We have found that hydrogen bonding and Lennard-Jones interactions in the MB model are sufficient to capture the thermodynamic properties of nonpolar solvation.[36]

The MB model allows continuous variation of the separations and orientations of water. Nonetheless it provides strong support for the two-state assumption that hydrogen bonds can be divided into the categories ''made'' and ''broken,'' like in the Muller model.[33] The MB model allows us to make a microscopic interpretation of the nature of made and broken H bonds in bulk water and in the solvation shells. A thermodynamic link to these calculated microscopic distributions is provided by the Muller model.

B. Review of the Muller model

Muller's model focuses on the hydrogen bonds among water molecules. H bonds occur in four possible states: intact in bulk water (BI), broken in bulk water (BB), intact in the first-neighbor shell of a nonpolar solute (SI), and broken in the first-neighbor shell around the solute (SB). Muller treats the transfer of a solute into water as a process in which n hydrogens that participated in hydrogen bonds in the bulk now become a part of the hydration shell of the solute. The resulting heat capacity change is

$$\Delta C_p = n(C_{p,\mathrm{shell}} - C_{p,\mathrm{bulk}}), \tag{6}$$

where $C_{p,\mathrm{shell}}$ and $C_{p,\mathrm{bulk}}$ are the heat capacity of the shell and bulk water molecules, respectively.

In Muller's model, the hydrogen bond breakage in bulk water is described as a two-state equilibrium,

$$\text{H bond (intact)} \Rightarrow \text{H bond (broken)}, \tag{7}$$

with equilibrium constant, K_{bulk},

$$K_{\mathrm{bulk}} = f_{\mathrm{bulk}}/(1-f_{\mathrm{bulk}}) = \exp(-\Delta H^{\circ}_{\mathrm{bulk}}/kT + \Delta S^{\circ}_{\mathrm{bulk}}/k), \tag{8}$$

where f_{bulk} is the fraction of hydrogen bonds broken, and k is the Boltzmann constant. The two states have a free energy difference $\Delta G^{\circ}_{\mathrm{bulk}} \equiv \Delta H^{\circ}_{\mathrm{bulk}} - T\Delta S^{\circ}_{\mathrm{bulk}}$, where $\Delta H^{\circ}_{\mathrm{bulk}}$ is the enthalpy of breaking a hydrogen bond in bulk water, and $\exp(\Delta S^{\circ}_{\mathrm{bulk}}/k)$ is the change in the degeneracy, i.e., the number of configurations that have a broken bond, relative to the intact form. In the Muller model, $\Delta H^{\circ}_{\mathrm{bulk}}$ and $\Delta S^{\circ}_{\mathrm{bulk}}$ are assumed to be independent of the temperature. Hence bond breaking contributes to the heat capacity, $\Delta C_{p,\mathrm{bulk}}$, in classical two-state fashion:[37]

$$\Delta C_{p,\mathrm{bulk}} = (\Delta H^{\circ}_{\mathrm{bulk}})^2 f_{\mathrm{bulk}}(1-f_{\mathrm{bulk}})/kT^2. \tag{9}$$

A similar hydrogen-bond-breaking equilibrium applies to water in the hydration shell of the solute:

$$K_{\mathrm{shell}} = f_{\mathrm{shell}}/(1-f_{\mathrm{shell}}) = \exp(-\Delta H^{\circ}_{\mathrm{shell}}/kT + \Delta S^{\circ}_{\mathrm{shell}}/k), \tag{10}$$

and

$$\Delta C_{p,\mathrm{shell}} = (\Delta H^{\circ}_{\mathrm{shell}})^2 f_{\mathrm{shell}}(1-f_{\mathrm{shell}})/kT^2. \tag{11}$$

C. Extension of the Muller model by Lee and Graziano

In addition to its effect on the heat capacity change, the transfer of a nonpolar solute into water will also change the enthalpy and entropy of the solution. Muller's original model assumed, for simplicity, that broken H bonds are the same whether they are in bulk water or in the solvation shell. However, since each broken H-bond state represents a distinct ensemble of configurations, one cannot assume they are the same. For instance, the presence of the solute may make the enthalpy (or entropy) of the shell broken state even more unfavorable (relative to the bulk broken state). To include this generality, Lee and Graziano[38] have extended the Muller model by assigning two additional parameters, $\Delta H^{\circ}_{\mathrm{distort}}$ and $\Delta S^{\circ}_{\mathrm{distort}}$, to reflect the extent to which the broken state in the shell is ''more broken'' (higher enthalpy) and of greater multiplicity (higher entropy) relative to the bulk broken state.

With these definitions, we define $\Delta H_{\mathrm{reorg}}$ and $\Delta S_{\mathrm{reorg}}$, the contributions that hydrogen bond reorganization makes to the enthalpy and entropy of transfer, to be

$$\Delta H_{\mathrm{reorg}} = n[\Delta H^{\circ}_{\mathrm{distort}} - (1-f_{\mathrm{shell}})\Delta H^{\circ}_{\mathrm{shell}} + (1-f_{\mathrm{bulk}})\Delta H^{\circ}_{\mathrm{bulk}}], \tag{12}$$

and

$$\Delta S_{\mathrm{reorg}} = n[\Delta S^{\circ}_{\mathrm{distort}} - (1-f_{\mathrm{shell}})\Delta S^{\circ}_{\mathrm{shell}} + (1-f_{\mathrm{bulk}})\Delta S^{\circ}_{\mathrm{bulk}} - k\Delta M], \tag{13}$$

respectively, where $k\Delta M \equiv k(M_{\mathrm{shell}} - M_{\mathrm{bulk}})$ is the mixing entropy with M_{bulk} and M_{shell} defined as

$$M_{\mathrm{bulk}} = f_{\mathrm{bulk}} \ln f_{\mathrm{bulk}} + (1-f_{\mathrm{bulk}})\ln(1-f_{\mathrm{bulk}}), \tag{14}$$

and

$$M_{\mathrm{shell}} = f_{\mathrm{shell}} \ln f_{\mathrm{shell}} + (1-f_{\mathrm{shell}})\ln(1-f_{\mathrm{shell}}). \tag{15}$$

Since Muller's model only includes information about the reorganization of the hydrogen bonds, it cannot be used directly to predict the full transfer thermodynamics. What is missing for a full determination of the transfer enthalpy is the binding energy, E_{bind}, of the solute in solution. E_{bind} is the ensemble-averaged total interaction of the solute with the surrounding solvent, and can be calculated directly from simulations. E_{bind} does not explicitly include the change in water–water interactions (although it is affected indirectly by water reorganization). With these definitions, the transfer enthalpy can be determined as the sum of its two contributions:

$$\Delta H_{\mathrm{tr}} = \Delta H_{\mathrm{reorg}} + E_{\mathrm{bind}}. \tag{16}$$

The entropy is more complicated. It cannot be formally separated into analogous contributions.[39] The effects of solute–solvent interactions are inextricably tied to the reorganization of water molecules. To first approximation, we will assume that most of the transfer entropy is absorbed in water reorganizations (i.e., $\Delta S_{\mathrm{reorg}} \cong \Delta S_{\mathrm{tr}}$). Note that $\Delta S_{\mathrm{reorg}}$ is hence *not* equivalent to other author's notion of ''solvent–solvent entropy,''[4,5,40] since our reorganizations include the direct perturbations induced by the solute.

The Muller model has five independent parameters (n, $\Delta H^{\circ}_{\mathrm{bulk}}$, $\Delta S^{\circ}_{\mathrm{bulk}}$, $\Delta H^{\circ}_{\mathrm{shell}}$, and $\Delta S^{\circ}_{\mathrm{shell}}$) to determine the transfer heat capacity change. The Lee and Graziano extension adds two additional parameters, $\Delta H^{\circ}_{\mathrm{distort}}$ and $\Delta S^{\circ}_{\mathrm{distort}}$, needed to fully determine the transfer enthalpy and entropy, respectively. The first parameter, n, the number of water hydrogens in the hydration shell, can be estimated on geometric grounds based on the surface area of the solute,[32] or obtained directly from simulation. In the past,[33,38] the quantities $\Delta H^{\circ}_{\mathrm{bulk}}$ and $\Delta S^{\circ}_{\mathrm{bulk}}$ have been estimated using the difference in heat capacity between steam and liquid water combined with the estimate of Pauling[41] for $f_{\mathrm{bulk}} = 0.15$ at 0 °C. Since the values for $C_{p,\mathrm{shell}}$ and f_{shell} are unknown, the remaining parameters in the original model, $\Delta H^{\circ}_{\mathrm{shell}}$ and $\Delta S^{\circ}_{\mathrm{shell}}$, were estimated by fitting to the hydration enthalpy, entropy, and heat capacities of nonpolar transfer. Lee and Graziano introduced $\Delta H^{\circ}_{\mathrm{distort}}$ and $\Delta S^{\circ}_{\mathrm{distort}}$ (which were assumed to be zero in Muller's treatment) to show that relatively small values for each could support their view of enthalpy–entropy compensation.[17,42,43] The main drawback of the Muller model and its variants are the many parameters that are freely adjustable.

D. Unambiguous parameter determination from the MB model

The overabundance of free parameters could be circumvented if the fraction of bulk and shell water molecules that are H bonded were known as a function of temperature. Computer simulations of the MB model yield this information.[36,44] Further, well-converged heat capacities and

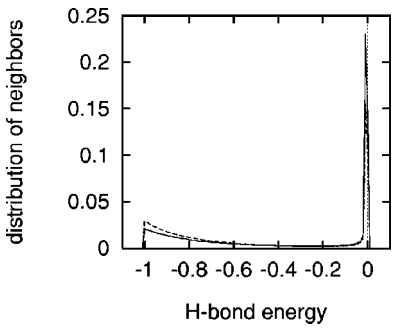

FIG. 2. Distribution of the hydrogen-bond energies (in units of $|\epsilon_{HB}|$, where ϵ_{HB} is the optimal hydrogen-bond energy) of neighboring water molecules in the bulk (solid line) and in the shell (dashed line) is bimodal for the MB model at all temperatures studied. The distribution shown is for $kT/|\epsilon_{HB}| = 0.18$, which is below T_S.

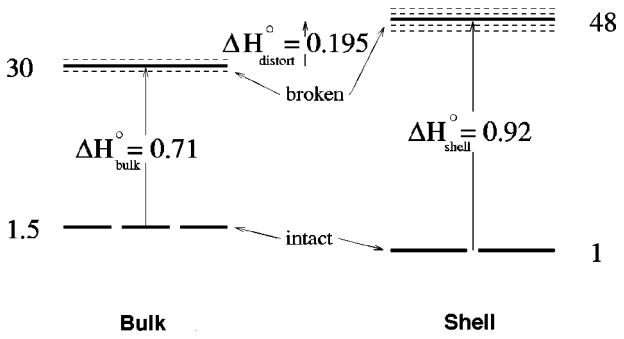

FIG. 3. Energy diagram of the extended Muller model that best fits the simulation data. Enthalpies are in units of the hydrogen bond, $|\epsilon_{HB}|$. The numbers next to each energy level indicate the relative degeneracy. (Since the absolute multiplicity is irrelevant, we have set the least degenerate state to 1.)

other thermodynamic properties can be calculated from the same set of simulations.[36] Hence the MB model can **both** test the two-state assumption **and** produce a consistent set of parameters for the Muller model. The procedure is as follows. (1) Least-squares fitting of the Monte Carlo simulations of the MB model to Eqs. (8) and (10) separately for the bulk and for the hydration shell then yields the energy gap and relative degeneracy parameters directly. These four parameters can then be used without alteration to predict the hydrogen-bond-breaking contribution to the heat capacity change. (2) The quantity $\Delta H^\circ_{distort}$ can then be determined from a direct fit to the reorganizational contribution to the total hydration enthalpy[42,45] using Eq. (12) and the other enthalpy parameters. (3) The remaining parameter, $\Delta S^\circ_{distort}$, can be approximated by fitting the transfer entropy to Eq. (13) (using the assumption that $\Delta S_{reorg} \cong \Delta S_{tr}$) once the other entropy parameters have been determined.

Our Monte Carlo simulations of the MB model show that water configurations fall into two distinct classes, which can reasonably be defined as having intact or broken hydrogen bonds. Figure 2 shows the distribution of energies for water neighbors in the shell and the bulk. This distribution is bimodal, indicating that the two-state approximation is valid in the MB model, and that it is meaningful to refer to ''intact'' and ''broken'' bonds, even though the hydrogen-bond energy function for the MB model is continuous and unimodal. The minimum in this bimodal function is very broad, so there is little sensitivity to how the cutoff that delineates intact from broken bonds is chosen. We have explored several cutoffs from 0.5 to 0.25 (in units of $|\epsilon_{HB}|$, where ϵ_{HB} is the optimal hydrogen bond energy), each yielding similar results for the Muller model parameters. We show results for a cutoff of 0.33, which is used throughout this article.

III. RESULTS FOR THE MB MODEL

A. Physical model of the hydrophobic effect

The microscopic basis of hydrophobicity is often taken to be ''water ordering around a nonpolar solute to avoid wasting hydrogen bonds.'' But such descriptions are seriously incomplete. Although the large positive free energy of mixing of hydrocarbons with water is dominated by entropy at 25 °C, it is dominated by enthalpy at higher temperatures (112 °C from Baldwin's extrapolation for hydrocarbons,[31,32] or 150 °C from the measurements of Crovetto *et al.* for argon[46]) where the disaffinity of oil for water is maximal. Therefore, where hydrophobicity is strongest, entropy plays no role. For this reason, models and simulations of solutes that focus only on cold water, around or below 25 °C, miss much of the thermodynamics of the oil/water solvation process.

The MB model yields a more complete description of the thermodynamics of hydrophobicity. We use the model of Muller, Lee, and Graziano (MLG) to extract from the results of the MB simulations a simple physical picture, which describes hydrophobicity thermodynamics in terms of just four physically interpretable energy levels, shown in Fig. 3.

The enthalpy and entropy parameters used to create this diagram were obtained by fitting the broken H-bond fractions in the bulk and in the shell. Figure 4 shows the fits. The temperature dependence of f_{bulk} and f_{shell} are shown in Fig. 4, along with the least-squares fit to the two-state model. The fit yields the following four parameter values for MB water: $\Delta H^\circ_{bulk} = 0.71$, $\Delta S^\circ_{bulk}/k = 2.99$, $\Delta H^\circ_{shell} = 0.92$, and $\Delta S^\circ_{shell}/k = 3.88$. The errors in fitting are quite small due to the excellent convergence of the simulations.

Here in Sec. III, we interpret the resulting energy-level diagram. The two main conclusions from Fig. 3 are that (1) inserting a nonpolar solute causes ordering of first-shell water molecules in cold water, but causes disordering of first-

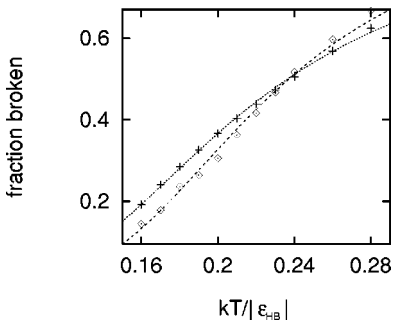

FIG. 4. Fraction of hydrogen bonds that are broken: hydration shell (◇), bulk (+). The lines are the best fit to the Muller model.

shell water molecules in hot water. (2) In cold water, the first-shell water molecules around a solute have a lower average hydrogen-bond energy than the water molecules surrounding a water molecule. The reverse is true in hot water.

To give a physical picture of these properties of the model, consider a central ''test'' molecule, either (i) a water molecule or (ii) a nonpolar solute molecule. Around the test molecule is an ensemble of all the possible configurations of first-shell waters. To a first approximation, the bonding of the ensemble of first-shell waters to second and more distant shells is the same whether the test particle is a water or a solute molecule, so we do not consider the second and outer shells further here. Levy and co-workers, in their solvation shell model, have given considerable justification for treating the thermodynamics using only the local surroundings of the test molecule.[5,7,47]

As a further simplification, suppose the Lennard-Jones part of the interaction is the same for water–water interactions as for water–solute interactions. This allows us to pay attention to only the hydrogen bonding contributions; they capture the essence of hydrophobicity in the MB model. Our focus is not on the central molecule. Rather, we focus on a water molecule in the first shell, and how its thermodynamic properties depend on whether the central molecule is a water or a solute. The left-hand side of Fig. 3 shows the energy diagram of a first-shell water when the central molecule is a water, and the right-hand side of Fig. 3 shows the energy diagram of a first-shell water when the central molecule is a nonpolar solute.

Irrespective of whether the central particle is a water or a solute molecule, heating weakens and breaks hydrogen bonds of the first-shell waters (either among themselves or with a central water), increasing the population in the higher (broken) energy level. Far fewer configurations have hydrogen bonds made than broken, so H-bond breakage leads to an increased entropy for the first-shell waters. In the MB model, bond breakage of the first-shell waters leads to a 20-fold increase in configurations when the central particle is water, or a 48-fold increase when the central particle is a solute. The two aspects of Fig. 3 that call for explanation, (i) Why are there *fewer* configurations of first-shell waters around a solute than around water at low T, and *more* configurations at high T? (ii) Why are first-shell hydrogen bonds ''better'' around a solute than around water at low T, and worse at high T?

The key to addressing these questions lies in recognizing that the class of ''made'' hydrogen bonds can be further subdivided into two subclasses. The best hydrogen bonding occurs among ''circumferential waters,'' which are first-shell water molecules that make hydrogen bonds to neighboring first-shell waters. Each circumferential water has the possibility of making two H bonds at a time to neighboring shell waters in the MB model. Circumferential waters cannot form a hydrogen bond to the central particle, so the energies of circumferential waters are relatively independent of whether the test particle is a water or a solute molecule. A second class of first-shell waters, called ''radial waters,'' points a hydrogen bond toward the central particle. On average, radial waters surrounding a central water molecule have higher

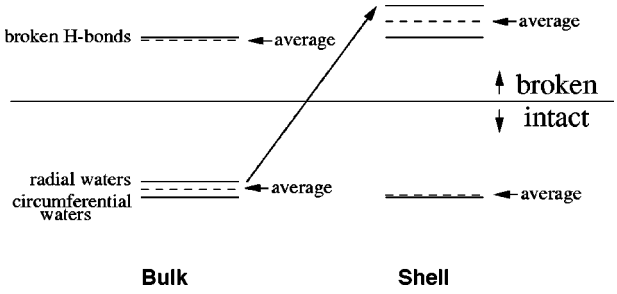

FIG. 5. Schematic energy diagram showing the effect on the energy levels if the test water molecule is changed to an isotropic solute.

H-bond energy than circumferential waters have, because a good H bond to the central water generally precludes another good H bond to a neighboring first-shell water. Recall that the premise of this simple picture of our MB results is that we can neglect, to first approximation, second and outer shells. Hence the only relevant H bonds are those of first-shell waters to other first-shell waters (or to the central molecule). The energy of a radial water in the first-shell depends strongly on whether the central molecule is a water or a nonpolar solute.

Now consider the process of replacing the central water molecule by a central nonpolar solute. The full ensemble of first-shell waters is the same in each case, but the Boltzmann factors differ. This exchange has little effect on circumferential waters, but a big effect on radial waters. Many of the radial water configurations now move up in energy, from the ''made'' to the ''broken'' class. (See Fig. 5 for a hypothetical depiction of the energy level shift induced by the solute–water replacement.) There are several consequences. First, as noted in the traditional arguments, fewer H-bonded configurations are possible around a nonpolar solute than around water, so the entropy decreases when nonpolar solutes are inserted into cold water.

Second, H bonds are ''better'' around a nonpolar solute, at low temperature, than around water, although only marginally. This is a statement about the ensemble average enthalpy of H bonds in the first-shell of water, not about individual H bonds. Around a water molecule, the first shell ''made'' hydrogen bonds come from both the strongly bound circumferential waters and from the weaker radial waters, giving an average intermediate strength. But the ''made'' hydrogen bonds around a nonpolar solute are predominantly due to circumferential waters, which are strong, hence the lower average H-bond enthalpies around a nonpolar solute than around water at low temperature. Previous simulations have led to conflicting conclusions about whether or not H bonds are better around nonpolar solutes.[1] We believe these conflicts may arise from (i) the marginal difference between bulk and shell H-bond strengths (which may be detectable only with sufficient conformational sampling) and (ii) the fact that most simulation studies do not distinguish H bonds within a shell versus those across the shell–bulk boundary, as we have done for the MB model.

So far, we have described the conclusions from Fig. 3 for cold water, where ground states dominate the behavior. In hot water (e.g., near the boiling temperature, and at higher

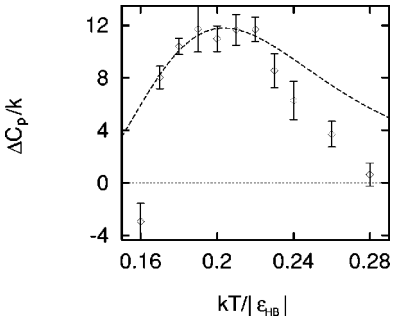

FIG. 6. Heat capacity as a function of temperature. Along with the simulation points ($\diamond$), the theoretical two-state prediction is shown (dotted line). Only the four parameters directly obtained from the hydrogen-bond fractions are used for the water-reorganization contribution to the heat capacity. The weak contribution from the solute–water interaction $\partial E_{\rm bind}/\partial T^* = 1.23$ (where $T^* = kT/|\epsilon_{\rm HB}|$) was added.

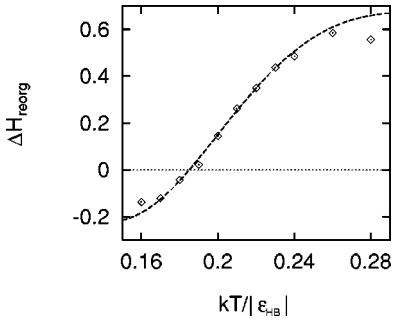

FIG. 7. Reorganization enthalpy (in units of $|\epsilon_{\rm HB}|$) plotted along with the two-state result. The points show the Monte Carlo results, and the line is the MLG model. The slope and shape of this curve are predetermined by the original four parameters. The additional parameter which describes the offset between the two sets of energy levels determines the intersection of the curve with the horizontal (reduced temperature) axis.

temperatures in compressed liquid water), the populations of the upper energy levels dictate the thermodynamics of hydrophobicity. The upper levels have just the opposite behavior of that of the lower levels: the entropy and enthalpy of the first-shell waters is higher around a solute than around water. Why is this so? Because the radial waters around a solute have high energy (broken H bonds), and there are many of them. Shifting from a central water to a central nonpolar solute leads to a shift of the radial waters from the ''made'' to the ''broken'' category, increasing the number of broken H-bond configurations and their average enthalpies.

B. Muller model predicts the Monte Carlo results well

We now test whether the Muller model, with its assumption of only four states, captures the essence of the hydrophobic heat capacity in the continuum-energy MB model. Do the four parameters obtained from fitting our Monte Carlo simulations give the correct configurational contribution to the transfer heat capacity change? Figure 6 shows that the Muller model works quite well. This is particularly remarkable since the heat capacity is a very sensitive function of such parameters. Note that the Muller model is not quantitatively accurate at very high or very low temperatures. At these extremes, the ensembles broaden and the two-state assumption breaks down. Adding additional states above the two upper states in the Muller model would reduce these errors.

IV. INTERPRETATION OF RESULTS FROM MC SIMULATIONS

A. Interpreting T_H and T_S

The points in Fig. 7 show the reorganizational enthalpy [the binding energy, as computed from the integral of (the solute–water energy)$\times$(the solute–water pair correlation function) at each temperature, has been subtracted from $\Delta H_{\rm tr}$]. The curve through the points in Fig. 7 is the MLG model where $\Delta H^{\circ}_{\rm distort} = 0.195$ is the free parameter we used to give the best fit with the Monte Carlo simulations. The quantity $\Delta H^{\circ}_{\rm distort}$, with the other parameters fixed, determines only the point at which the curve crosses zero; otherwise it has no effect on the shape of the curve.

The model allows us to interpret T_H, the temperature at which the enthalpy of solute transfer is zero. At low temperatures $\Delta H_{\rm reorg} < 0$. This implies that the insertion of solute and the attendant creation of a solvation shell in water lead to better hydrogen bonding. Thus, in cold water, solute insertion induces a shell of good hydrogen bonding. But solute insertion into hot water has the opposite effect: introducing a nonpolar solute produces a shell of hydrogen bonds that is worse than in the corresponding bulk water solvent. The temperature T_H at which $\Delta H_{\rm tr} = 0$ is a point of ideality where the reorganizational enthalpy balances the solute–solvent energy, $\Delta H_{\rm reorg} = -E_{\rm bind}$.

At present, it is not clear from conventional three-dimensional (3D) water simulations whether or not $\Delta H_{\rm reorg} < 0$ at low temperatures. Some 3D water models give results that are in agreement with the MB model (e.g., Ref. 5); others do not.[48] It should be noted that the qualitative picture we have described in Sec. III A implies a negative $\Delta H_{\rm reorg}$ at low temperature. We have found that parameters for Muller's model derived from real 3D water spectroscopic experiments give $\Delta H_{\rm reorg}$ (and all derived parameters), in qualitative agreement with our study here.[49]

Figure 8 shows the entropy of transfer. The best fit value is $\Delta S^{\circ}_{\rm distort}/k = 0.46$. For the entropy, there is no equivalent of $E_{\rm bind}$, so the transfer entropy is identical to the reorganizational entropy, and T_S is the temperature at which that en-

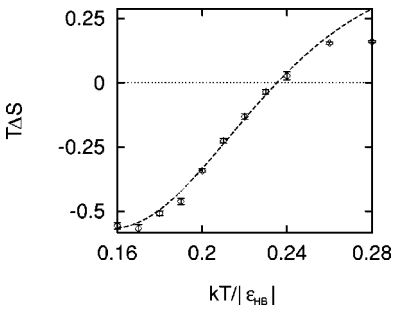

FIG. 8. Transfer entropy ($T\Delta S$) in units of $|\epsilon_{\rm HB}|$ (points) plotted along with the two-state result (dotted line). The slope and shape of this curve are predetermined by the original four parameters. The additional parameter which describes the relative degeneracies of the upper energy levels in each set determines the intersection of the curve with the x axis.

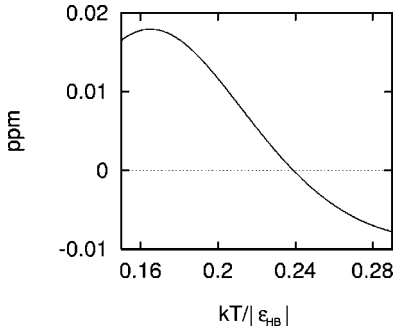

FIG. 9. Predicted NMR chemical shift as a function of reduced temperature with the assumptions discussed in the text.

tropy equals zero. As we have stated in an earlier work,[36] we have found that T_S is the point at which shell and bulk water molecules around a solute reverse their roles in hydrogen bonding (compare the crossing temperatures in Figs. 4 and 8 of this work).

The parameter $\Delta S^{\circ}_{\text{distort}}$, coupled with $\Delta S^{\circ}_{\text{shell}}$ and $\Delta S^{\circ}_{\text{bulk}}$, form a self-consistent set shown in Fig. 3. One out of every three H bonds breaks as a central water is replaced by a central nonpolar solute. Lee[17,38,42] and others[5,40,50–52] have argued that the reorganizational entropy should compensate the corresponding enthalpic term nearly exactly. The value of $\Delta S^{\circ}_{\text{distort}}$ which would most closely realize this expectation $(0.88k)$ would imply roughly equal numbers[53] of hydrogen-bonding states in the bulk and in the hydration shell. This, however, is inconsistent with our qualitative picture.

B. Crossover temperatures for other properties

The enthalpy and entropy of transfer are not the only properties that have a crossover temperature in the liquid range of water. Muller noted that the NMR chemical shift changes sign with temperature. A downfield shift is taken to indicate enhanced hydrogen bonding. Downfield shifts are observed at low temperatures, but upfield shifts are observed at higher temperatures. The implication is that solvation shell hydrogen bonds are not stronger than bulk hydrogen bonds at all temperatures. Muller described the relationship between chemical shift, $\Delta\delta$, and the fraction of broken hydrogen bonds with the expression,

$$\Delta\delta/m=(n/111.1)[B(1-f_{\text{shell}})-A(1-f_{\text{bulk}})], \qquad (17)$$

where m is the molality of the solute in water and A and B are the downfield chemical shifts that result from hydrogen bonds in the bulk and in the shell, respectively. Although our parameters are quite different from Muller's, Fig. 9 shows that our model also suitably accounts for this behavior. For simplicity, we have assumed that $A=B$, and that both have the value of 5.5 ppm that Muller estimated from values given in the literature. Increasing the value of B relative to that of A shifts the crossing temperature to the right.

Our model predicts a crossover temperature below which shell H bonds are more populated than bulk H bonds, and above which the reverse holds. In contrast, the original Muller parameters predict that bulk H bonds are more populated at all temperatures. In that regard, we believe the

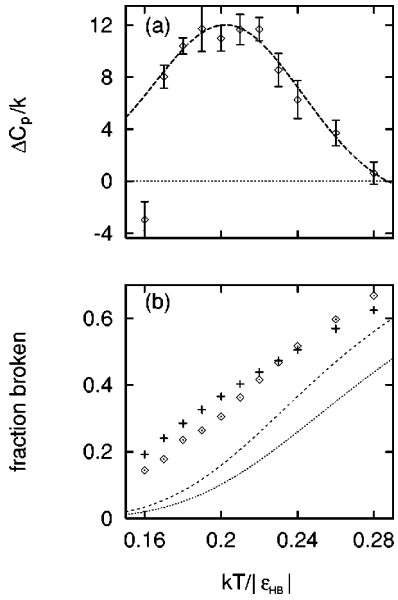

FIG. 10. Demonstration that (a) overfitting the heat capacity leads to (b) the very same qualitative conclusion—that more shell H bonds are broken than bulk ones at all temperatures—as Muller's original parameterization. The curves in (b) show the Muller model predictions (i.e., parameters determined directly from a fit to the transfer heat capacity) for broken shell (dashed lines) and bulk (dotted lines) H bonds. The points show the actual MB shell ($\diamond$) and bulk ($+$) values for comparison.

Muller parameters are nonphysical. They are inconsistent with results of all-atom simulations.[6,54,55] Muller chose to fit the heat capacity of hydration rather than the curves for f_{bulk} and f_{shell}. (Figure 10 shows a least-squares fit to the MB heat capacity to derive the parameters, rather than fitting f_{bulk} and f_{shell} directly). We believe it is more consistent with the logic of the model to fit f_{bulk} and f_{shell}, and then use them to predict the heat capacity.

V. CONCLUSIONS

We have used the MB model, a statistical mechanical model of water, to explore the principles of hydrophobic solvation. We have found that the four-state Muller model, as modified by Lee and Graziano, accounts well for the thermodynamic temperature trends of hydrophobic transfers in the MB model of water. The Muller model approximates solvation using two states, hydrogen bonds are made or broken, in the bulk and in the solvation shell. The primary parameters are an enthalpy gap and the relative degeneracy of states for both the hydration shell and the bulk. We have obtained these parameters using a microscopic model from the fraction of broken bonds observed in MB water simulations. Using the framework of the Muller model, these parameters are used without adjustment to predict transfer heat capacities over a range of temperatures. These predictions are in reasonable agreement with direct heat capacity measurements from MB water (calculated on the same set of simulations from which the H-bond fractions were tabulated).

A consistent physical picture is described that accounts for the qualitative difference observed between shell and bulk parameters. This picture focuses on the differences be-

tween water molecules in the shell of a solute versus those that surround an ordinary water. The model gives a physical interpretation for T_H and T_S, the temperatures at which the transfer enthalpy and entropy, respectively, are zero. T_H is the temperature at which H-bond reorganizations are balanced by solute–solvent interactions. T_S is the temperature at which the relative H-bonding strengths and numbers of shell and bulk water molecules reverse roles.

ACKNOWLEDGMENTS

One of the authors (K.A.T.S.) gratefully acknowledges support by a U.S. National Science Foundation graduate research fellowship and a University of California, San Francisco, Regent's fellowship. The authors thank the NIH for support. Some calculations in this article were performed at the SydCom, the USyd/UTS Distributed Computing Facility, supported by the Australian Research Council (ARC) (Grant No. A29530010), to whom acknowledgment is made. They thank Michael Johnson for setting up his nonlinear least-squares program (NONLIN) on our system, and Karen Tang for her insightful contributions in providing a physical interpretation of our double-two-state parameters.

APPENDIX: EXHAUSTIVE GRID ENUMERATIONS OF FEW-BODY SYSTEMS

In this Appendix, we use the MB model to study another property of hydrophobic solvation. We explore the multibody nature of water–water interactions, in pure water and around solutes. Hydrophobic solvation has been modeled using various different levels of approximation. One is pair interactions.[56,57] Another approach treats hydrophobic solvation as a property of the ''tetrahedrality'' of water, implying the importance of three-body or four-body arrangements of water molecules.[58] A third approach views hydrophobicity as resulting from polyhedral clathrate cages,[59,60] implying that six- or higher-body effects might be important. Such polyhedra have also been found in the MB model.[36] The key question is, What is the minimum number of water molecules needed to account for the essential physics of hydrophobic solvation?

We have performed few-body exhaustive grid enumerations to address this question and to distinguish among the above approximations. We enumerate all relative orientations and separations of two model water molecules on a grid. We then systematically add additional water molecules one at a time and enumerate their contributions to the partition function by similar exhaustive grid enumeration.

To do this, we fix a first MB water molecule in space. A second water molecule is added to the system and moved in fixed increments in the xy coordinate system. Water number two is constrained to be within a neighboring distance from the first (i.e., within the first minimum of the water–water pair correlation function, $g_{\mathrm{WW}}(r)$, as determined from previous full Monte Carlo simulations). At each relative position, the angles of each molecule are sampled in fixed increments (the grid size is made small enough so that subsequent reductions cause no changes in the relative distributions obtained) from 0° to 120° (this upper limit is dictated by the molecular symmetry).

We evaluate Eqs. (A1)–(A4) from our grid enumerations. When a solute is present, the fixed reference water is always within its hydration shell [i.e., the solute and fixed water are separated by a distance within the first minimum in the solute–water pair correlation function, $g_{\mathrm{SW}}(r)$]. Each water molecule that is added to the system must be a neighbor of an existing water, so that the system remains contiguous (i.e., if water molecules are the nodes of a graph, and if edges indicate joined neighbors, the graph is connected).

In practice, computer limitations prevent us from performing the exhaustive grid enumerations for more than four molecules. To go beyond that limit, we performed Boltzmann-weighted sampling (i.e., Metropolis Monte Carlo) on systems from 2 to 12 water molecules (with and without a solute), without periodic boundary conditions, but with the same connectivity requirements around a fixed reference water as above.

We can use these few-body MB simulations to make an estimate of Muller's parameters by an alternative strategy. Our motivation will be (i) to validate the parameters derived by the fits to the H-bond fractions and (ii) to determine how many molecules are needed to regain the enthalpy gaps and degeneracies from the full Monte Carlo simulations.

We bin the total energy of a configuration into two classes, depending upon the H-bonded status of a chosen pair of water neighbors (adding one entry of the total system energy based upon each pair of neighboring water molecules in the system). The distributions for ''intact'' and ''broken'' H-bonded pairs are then separately Boltzmann weighted to yield the average energy and entropy. For example, the average energy and entropy for the distribution corresponding to the intact H bonds in the bulk (BI) are

$$\langle E_{BI}\rangle = \sum_{\epsilon} \epsilon\Omega(\epsilon)\exp(-\epsilon/kT) \Big/ \sum_{\epsilon} \Omega(\epsilon)\exp(-\epsilon/kT), \tag{A1}$$

$$\langle S_{BI}/k\rangle = \langle E_{BI}\rangle/kT + \ln\left[\sum_{\epsilon} \Omega(\epsilon)\exp(-\epsilon/kT)\right], \tag{A2}$$

where the sums are performed over the energy bins or levels, ϵ, and $\Omega(\epsilon)$ is the density of states obtained from the enumeration. Similar calculations are performed for states BB, SI, and SB. Taking the differences of these quantities yields the parameters needed for the Muller model:

$$\begin{aligned} \Delta H^{\circ}_{\mathrm{bulk}}(T) &= \langle E_{BB}\rangle - \langle E_{BI}\rangle, \\ \Delta H^{\circ}_{\mathrm{shell}}(T) &= \langle E_{SB}\rangle - \langle E_{SI}\rangle, \end{aligned} \tag{A3}$$

$$\begin{aligned} \Delta S^{\circ}_{\mathrm{bulk}}(T) &= \langle S_{BB}\rangle - \langle S_{BI}\rangle, \\ \Delta S^{\circ}_{\mathrm{shell}}(T) &= \langle S_{SB}\rangle - \langle S_{SI}\rangle. \end{aligned} \tag{A4}$$

(We are assuming that the change in volume associated with breaking a H bond is small, so we can equate energies with enthalpies.) Whereas the Muller model assumes that the

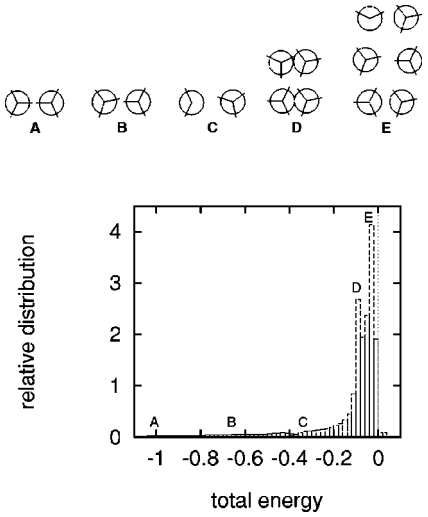

FIG. 11. Relative distribution of intact (solid lines) and broken (dashed lines) H-bonded states for the enumeration of two MB water molecules. Representative configurations at various energies are shown above the distribution of states. Note that, although the orientations of the pair of waters in B is the same as the middle pair in E, the larger intermolecular separation in E leads to weak interactions.

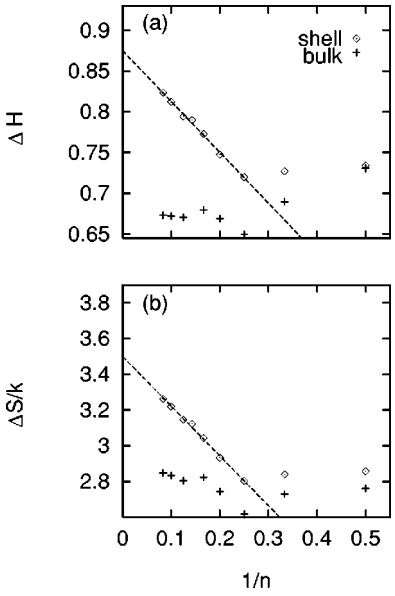

FIG. 13. Progression of (a) $\Delta H°$ and (b) $\Delta S°/k$ as a function of the reciprocal number of water molecules $(1/n)$ for the hydration shell $(\diamond)$ and the bulk $(+)$, all at $kT/|\epsilon_{\mathrm{HB}}|=0.18$.

quantities $\Delta H°$ and $\Delta S°$ in Eqs. (A3) and (A4) do not depend on temperature, they do in the MB model, but only weakly.

Treating our Monte Carlo simulations as the ''true'' or ''exact'' behavior of MB water, we can now ask how closely two-body or three-body approximations will come to predicting the true behavior of the model water. We find that the two-body approximation is remarkably good for predicting the properties of pure bulk water ($\Delta H^{\circ}_{\mathrm{bulk}}=0.71$ and $\Delta S^{\circ}_{\mathrm{bulk}}/k=2.7$, from both the exhaustive grid enumeration and the Boltzmann-weighted sampling) compared to $\Delta H^{\circ}_{\mathrm{bulk}}=0.71$ and $\Delta S^{\circ}_{\mathrm{bulk}}/k=2.99$ from the full Monte Carlo simulation. The unweighted distribution of two-body states is shown in Fig. 11 along with examples of intact and broken configurations. The underestimate at the two-body level in the relative entropy of broken to intact H-bonded states implies that there are more intact states in the two-body approximation than in the many-body simulations. The presence of more intact states leads to an *overestimate* in the H-bonded order (see Fig. 12) relative to the full simulation, which is most pronounced at low temperatures. This trend is observed and described elsewhere in a formal theoretical expansion of the entropy of MB water.[61]

While the two-body approximate partition function yields a reasonable model for bulk water, it is not sufficient for nonpolar solvation. Nonpolar solvation is not well approximated by two-body or three-body terms. A nearly full solvation shell, four to six water molecules plus the solute, is required to approximate the correct trends in the solvation parameters. A full second shell offers further improvement, but since the discrepancies appear to diminish with the number, n, of water molecules linearly as $1/n\rightarrow\infty$ (see Fig. 13), it seems that even distant water molecules contribute, to a small degree, to nonpolar solvation.

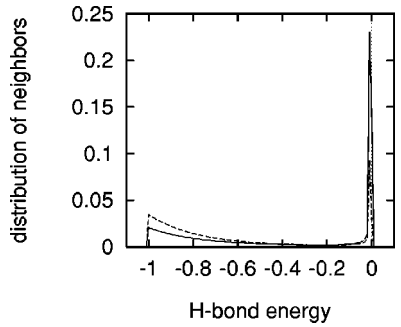

FIG. 12. Distribution of hydrogen-bond energies at a low temperature $(kT/|\epsilon_{\mathrm{HB}}|=0.18)$ for the full simulation (solid line) and for the two-water system (dashed line).

[1] W. Blokzijl and J. B. F. N. Engberts, Angew. Chem. Int. Ed. Engl. **32**, 1545 (1993).
[2] S.-B. Zhu, S. Singh, and G. W. Robinson, Adv. Chem. Phys. **85**, 627 (1994).
[3] For work in this area prior to 1993, see Refs. 1 and 2, and references therein.
[4] B. Guillot and Y. Guissani, J. Chem. Phys. **99**, 8075 (1993).
[5] N. Matubayasi, L. H. Reed, and R. M. Levy, J. Phys. Chem. **98**, 10640 (1994).
[6] R. L. Mancera and A. D. Buckingham, J. Phys. Chem. **99**, 14632 (1995).
[7] N. Matubayasi and R. M. Levy, J. Phys. Chem. **100**, 2681 (1996).
[8] S. Garde, G. Hummer, A. E. Garćia, M. E. Paulaitis, and L. R. Pratt, Phys. Rev. Lett. **77**, 4966 (1996).
[9] J. W. Arthur and A. D. J. Haymet, J. Chem. Phys. **109**, 7991 (1998).
[10] J. W. Arthur and A. D. J. Haymet, J. Chem. Phys. **110**, 5873 (1999).
[11] L. R. Pratt and D. Chandler, J. Chem. Phys. **67**, 3683 (1977).
[12] L. R. Pratt, Annu. Rev. Phys. Chem. **36**, 433 (1985).
[13] F. Hirata, B. M. Pettitt, and P. J. Rossky, J. Chem. Phys. **77**, 509 (1982).
[14] A. Tani, Mol. Phys. **48**, 1229 (1983).
[15] R. A. Pierotti, Chem. Rev. **76**, 717 (1976).
[16] K. Soda, J. Phys. Soc. Jpn. **58**, 8643 (1989).
[17] B. Lee, Biopolymers **31**, 993 (1991).
[18] K. Soda, J. Phys. Soc. Jpn. **62**, 1782 (1993).
[19] B. J. Berne, Proc. Natl. Acad. Sci. USA **93**, 8800 (1996).
[20] W. G. Schneider, H. J. Bernstein, and J. A. Pople, J. Chem. Phys. **28**, 601 (1958).
[21] N. Muller and R. C. Reiter, J. Chem. Phys. **42**, 3265 (1965).

[22] N. Muller, J. Chem. Phys. **43**, 2555 (1965).
[23] J. C. Hindman, J. Chem. Phys. **44**, 4582 (1966).
[24] A. K. Soper and J. Turner, Int. J. Mod. Phys. B **7**, 3049 (1993).
[25] B. Madan and K. Sharp, J. Phys. Chem. **100**, 7713 (1996).
[26] K. A. Sharp and B. Madan, J. Phys. Chem. B **101**, 4343 (1997).
[27] M. G. Sceats, M. Stavola, and S. A. Rice, J. Chem. Phys. **70**, 3927 (1979).
[28] M. G. Sceats and S. A. Rice, J. Chem. Phys. **72**, 6183 (1980).
[29] S. A. Rice and M. G. Sceats, J. Phys. Chem. **85**, 1108 (1981).
[30] A. R. Henn and W. Kauzmann, J. Phys. Chem. **93**, 3770 (1989).
[31] R. L. Baldwin, Proc. Natl. Acad. Sci. USA **83**, 8069 (1986).
[32] P. L. Privalov and S. J. Gill, Adv. Protein Chem. **39**, 191 (1988).
[33] N. Muller, Acc. Chem. Res. **23**, 23 (1990).
[34] D. Eisenberg and W. Kauzmann, *The Structure and Properties of Water* (Oxford University Press, Oxford, 1969), pp. 256–265; G. Nemethy and H. A. Scheraga, J. Chem. Phys. **36**, 3401 (1962).
[35] A. Ben-Naim, J. Chem. Phys. **54**, 3682 (1971).
[36] K. A. T. Silverstein, A. D. J. Haymet, and K. A. Dill, J. Am. Chem. Soc. **120**, 3166 (1998).
[37] S. J. Gill, S. F. Dec, G. Olofsson, and I. Wadso, J. Phys. Chem. **89**, 3758 (1985).
[38] B. Lee and G. Graziano, J. Am. Chem. Soc. **118**, 5163 (1996).
[39] Y.-Y. Shi, A. E. Mark, W. Cun-Xin, H. Fuhua, H. J. C. Berendsen, and W. F. van Gunsteren, Protein Eng. **6**, 289 (1993).
[40] H.-A. Yu and M. Karplus, J. Chem. Phys. **89**, 2366 (1988).
[41] L. Pauling, *The Nature of the Chemical Bond*, 3rd ed. (Cornell University Press, Ithaca, NY, 1960), p. 468.
[42] B. Lee, Biopolymers **24**, 813 (1985).
[43] R. Lumry, E. Battistel, and C. Jolicoeur, Faraday Symp. Chem. Soc. **17**, 93 (1982).
[44] While the fraction of bulk H bonds can be obtained directly by dividing the bulk-water H-bond coordination number by the number of arms per water molecule (three in the MB model), the shell H-bond fraction is more complicated. This is because, on average, one of the arms of a shell molecule will be pointing outward into the bulk medium, while the remaining two arms are pointing into the shell. We want to exclude the effects of the arm pointing toward the bulk. To do this, we take the shell H-bond coordination value and subtract one third of the bulk H-bond coordination value. What remains is the average H-bond coordination of the two arms of interest. Dividing this quantity by two (for the two arms pointing towards the shell) gives us the fraction of intact H bonds that is actually in the hydration shell $(1-f_{\text{shell}})$. We could also have obtained the shell H-bond fraction by keeping track of only the interactions of neighboring waters that are both in the shell.
[45] B. Guillot, Y. Guissani, and S. Bratos, J. Chem. Phys. **95**, 3643 (1991).
[46] R. Crovetto, R. Fernández Prini, and M. L. Japas, J. Chem. Phys. **76**, 1077 (1982).
[47] N. Matubayasi, E. Gallicchio, and R. M. Levy, J. Chem. Phys. **109**, 4864 (1998).
[48] S. R. Durell and A. Wallqvist, Biophys. J. **71**, 1695 (1996).
[49] K. A. T. Silverstein, A. D. J. Haymet, and K. A. Dill (unpublished).
[50] A. Ben-Naim, Biopolymers **14**, 1337 (1975).
[51] K. Soda, J. Phys. Soc. Jpn. **63**, 814 (1994).
[52] H. S. Ashbaugh and M. E. Paulaitis, J. Phys. Chem. **100**, 1900 (1996).
[53] Beginning with the least degenerate state (the intact hydration shell level) and moving clockwise in Fig. 3, the relative number of states at the four levels would be 1:1:20:48 to satisfy a nearly complete compensation criterion.
[54] A. Geiger, A. Rahman, and F. H. Stillinger, J. Chem. Phys. **70**, 263 (1979).
[55] S. Okazaki, K. Nakanishi, H. Touhara, N. Watanabe, and Y. Adachi, J. Chem. Phys. **74**, 5863 (1981).
[56] T. Lazaridis and M. E. Paulaitis, J. Phys. Chem. **96**, 3847 (1992).
[57] T. Lazaridis and M. E. Paulaitis, J. Phys. Chem. **98**, 635 (1994).
[58] N. Matubayasi, J. Am. Chem. Soc. **116**, 1450 (1994).
[59] G. Alagona and A. Tani, J. Chem. Phys. **72**, 580 (1980).
[60] T. Head-Gordon, Proc. Natl. Acad. Sci. USA **92**, 8308 (1995).
[61] K. A. T. Silverstein, K. A. Dill, and A. D. J. Haymet (unpublished).